AN OVERVIEW OF EXTREME EVENT ATTRIBUTION

Richard L. Smith

Joint Statistical Meetings

Nashville, August 7, 2025.

THE UNIVERSITY
of NORTH CAROLINA
at CHAPEL HILL

FOUNDED 1894
VOLUME 161, No. 162

FACEBOOK.COM/NEWSANDOBSERVER
TWITTER.COM/NEWSOBSERVER

NEWS ALL DAY.
YOUR WAY.

TUESDAY JULY 8 2025

$3.00

The News&Observer

NEWSOBSERVER.COM

TRAVIS LONG tlong@newsobserver.com

A water rescue unit paddles a raft in the Old Farm neighborhood along the Eno River in Durham on Monday morning, after Tropical Storm Chantal caused flash flooding.

Chapel Hill flooding displaces over 60, ravages businesses

BY TAMMY GRUBB
tgrubb@newsobserver.com

Chapel Hill business owners and residents woke up Monday to nearly 200 flooded cars, busted storefronts and mud and debris left behind by a 3- to-5-foot wall of water delivered by Tropical Storm Chantal.

The town evacuated more than 60 people from several apartment complexes overnight.

At Eastgate Crossing Shopping Center and University Place mall, restoration crews were taking stock of the damage and assessing the next steps for cleanup and repairs. A Chapel Hill police officer was patrolling Eastgate Crossing, on the lookout for looters after some were reported entering through bro-

The "Big Picture" Question

Extreme events such as Tropical Storm Chantal or the recent Texas floods are often said to be "caused by" global warming

- What does this mean?
- How can we quantify the relationship?
- What is the uncertainty?

Outline of Talk

I Detection and Attribution

- For means
- For extremes

II Overview of Extreme Value Theory

III Methods of Extreme Event Attribution

IV World Weather Attribution

V Alternative Methods

VI Examples

https://rls.sites.oasis.unc.edu/s834-2025/SmithDetectionAttributionPreprint.pdf

I. Detection and Attribution

(b) Change in global surface temperature (annual average) as **observed** and simulated using **human & natural** and **only natural** factors (both 1850–2020)

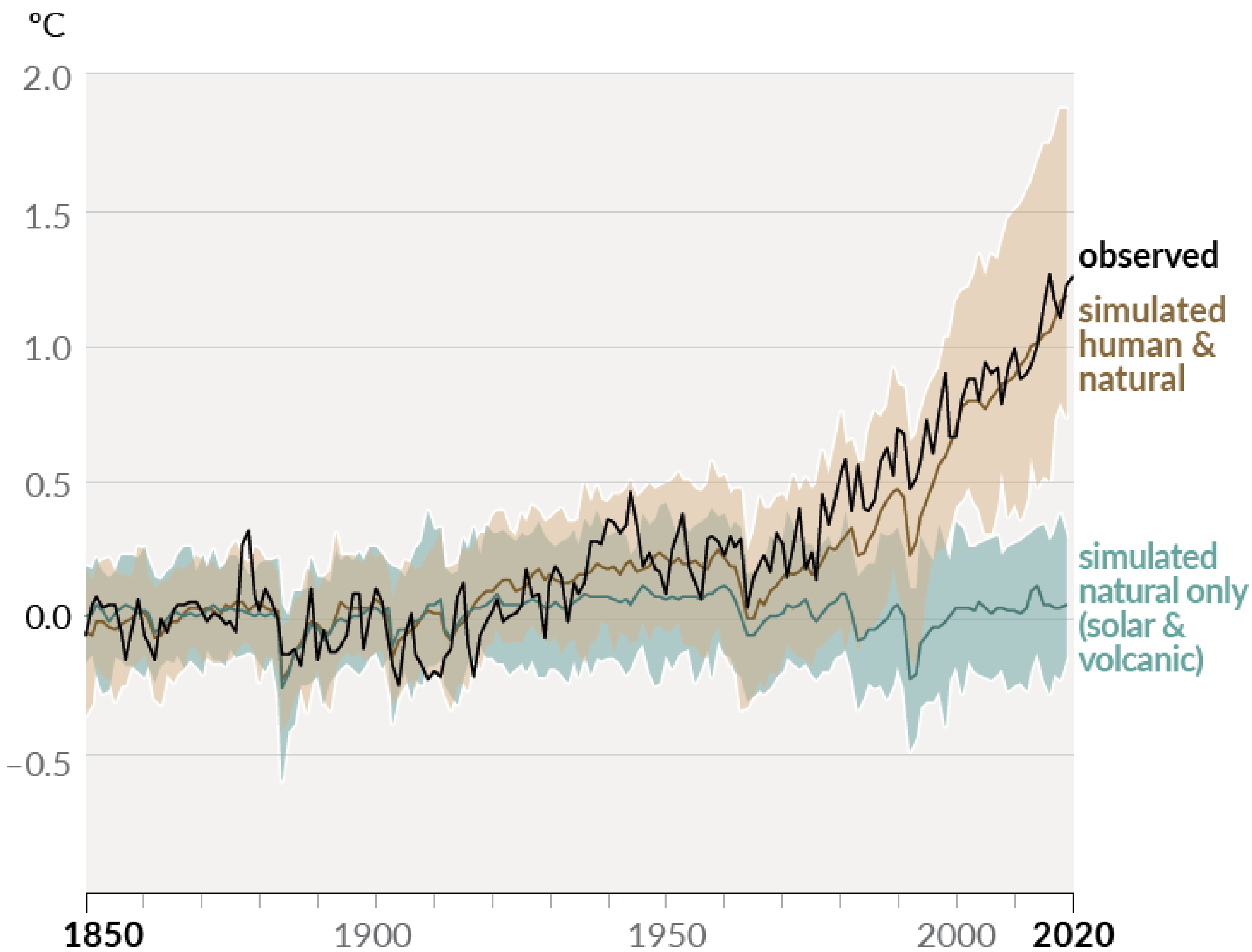

IPCC Sixth Assessment Report (2021)

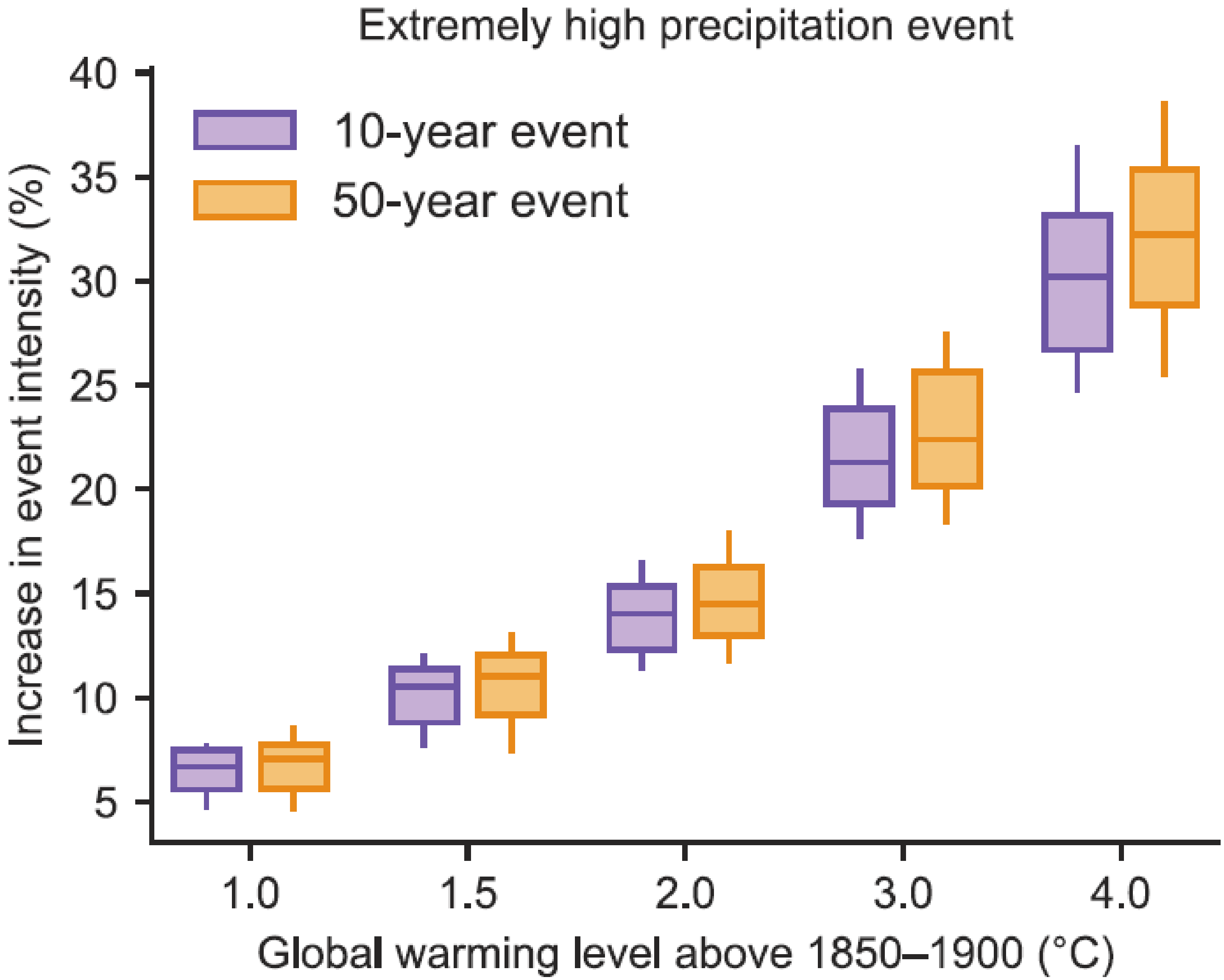

Figure 11.15 | Projected changes in the intensity of extreme precipitation events under 1°C, 1.5°C, 2°C, 3°C, and 4°C global warming levels relative to the 1850–1900 baseline. Extreme precipitation events are defined as the annual

IPCC Sixth Assessment Report (2021)

Summary of Detection/Attribution

- For means:
  - Regression of observational signal on "anthropogenic" and "natural" climate model signals
  - "Detection" means the anthropogenic component is statistically significant
  - "Attribution" measures the size of that component compared with natural signals and interval variability

- For extremes:
  - Define the extreme events we are interested in
  - Focus on *either* change in probability for a given magnitude *or* change in magnitude for a given probability
  - Use *extreme value theory* to assess magnitude and statistical significance of changes

II. Overview of Extreme Value Theory

Extreme Value Distributions

- Generalized Extreme Value distribution (GEV):

$$G(y) \;=\; \exp\left\{ -\left(1+\xi\frac{y-\mu}{\sigma}\right)_{+}^{-1/\xi} \right\} \qquad \left[x_{+} \;=\; \max(x,0) \right]$$

- Applied to annual or seasonal maxima
- Generalized Pareto distribution (GPD):

$$G(y) \;=\; 1-\left(1+\xi\frac{y}{\eta}\right)_{+}^{-1/\xi}$$

- Applied to exceedances over a threshold (usually need a separate model for the probability of exceeding the threshold)
- There are a number of variants of these models, with names like the "r-largest order statistics model" or the "point process model" (featured later)
- Any of the parameters may be extended to include covariates
- Estimation usually achieved through maximum likelihood or Bayesian techniques

Example

- GEV for time-dependent extremes: in year t,

$$G_t(y) \quad = \quad \exp\left\{-\left(1+\xi_t \frac{y-\mu_t}{\sigma_t}\right)_+^{-1/\xi_t}\right\}$$

- Hurricane Harvey led to extreme multi-day rainfall events in an area round Houston, Texas

- Risser and Wehner (2017) applied this model to annual maxima 7-day rainfalls over the hurricane season

- Covariates
  - Log of total atmospheric CO_2
  - Niño 3.4 index

- μ_t and $\log \sigma_t$ assumed to depend linearly on covariates; ξ_t treated as constant

- Concept of Granger causality

- Conclusion? "...human-induced climate change likely increased the chances of the observed precipitation accumulations during Hurricane Harvey in the most affected areas of Houston by a factor of at least 3.5."

III. Methods of Extreme Event Attribution

- Two National Academies reports (2016 and forthcoming)

- Original formulation of "fraction of attributable risk" (Stott, Stone and Allen, 2004)

$$FAR = \frac{p_1 - p_0}{p_0}$$

  where p_1 and p_0 are probabilities of the extreme event under all-forcings and natural-forcings respectively (or "present-day" and "pre-industrial")

- Alternative: risk ratio $RR = \frac{p_1}{p_0}$

- EVT versus "counting" techniques

- Causality, e.g. Granger versus Pearl

- Conditioning

- Selection bias

IV. World Weather Attribution

https://www.worldweatherattribution.org/

Growing exposure and uncertain rainfall trends highlight the critical need for climate resilience in Colombia and Venezuela

Latest analyses

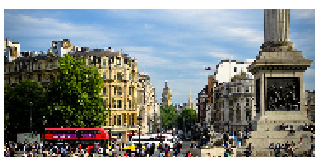

Heatwave

Climate change turns warm summer days in England into health threat

A high-pressure system over southern

Heatwave

Climate change drives record-breaking heat in Iceland and Greenland challenging cold adapted ecosystems and societies

Extreme rainfall

Mixed rainfall trends highlight the importance of climate adaptation in coastal New South Wales

Heatwave

Heatwaves can be particularly dangerous to humans, and occur all over the world with increasing intensity.

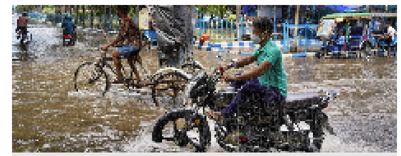

Extreme rainfall

Rainfall events from a major storm or hurricane, or intense localised downpours can lead to flooding in any type of location.

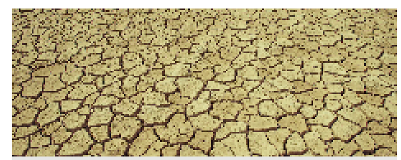

Drought

Drought affects people in many ways, from reduced water & food supplies to increasing the risk of wildfires.

Wildfire

- A group of meteorologists, statisticians and computer experts based in the U.K. and Netherlands
- Publish reports on extreme weather events as quickly as possible after the event occurred
- Typical conclusion: "This event was x [fill in your favorite value of x] times more likely to occur in present-day climate than it would have been under pre-industrial conditions"
- Alternatively: "The temperature/precipitation/windspeed was x degrees/ millimeters/meters per second higher than an event with the same return period in pre-industrial times"
- Data from observations and from climate models under both present-day and historical conditions
- Wide variety of statistical methods, but particularly EVT
- Examples:
  - Pacific northwest heatwave of 2021
  - Los Angeles wildfires of January 2025

Rapid attribution analysis of the extraordinary heat wave on the Pacific coast of the US and Canada in June 2021

Sjoukje Y. Philip[1,★], Sarah F. Kew[1,★], Geert Jan van Oldenborgh[1,2,✝], Faron S. Anslow[3], Sonia I. Seneviratne[4], Robert Vautard[5], Dim Coumou[1,6], Kristie L. Ebi[7], Julie Arrighi[8,9,10], Roop Singh[8], Maarten van Aalst[8,9,11], Carolina Pereira Marghidan[9], Michael Wehner[12], Wenchang Yang[13], Sihan Li[14], Dominik L. Schumacher[4], Mathias Hauser[4], Rémy Bonnet[5], Linh N. Luu[1], Flavio Lehner[15,16], Nathan Gillett[17], Jordis S. Tradowsky[18,19], Gabriel A. Vecchi[13,20], Chris Rodell[21], Roland B. Stull[21], Rosie Howard[21], and Friederike E. L. Otto[14]

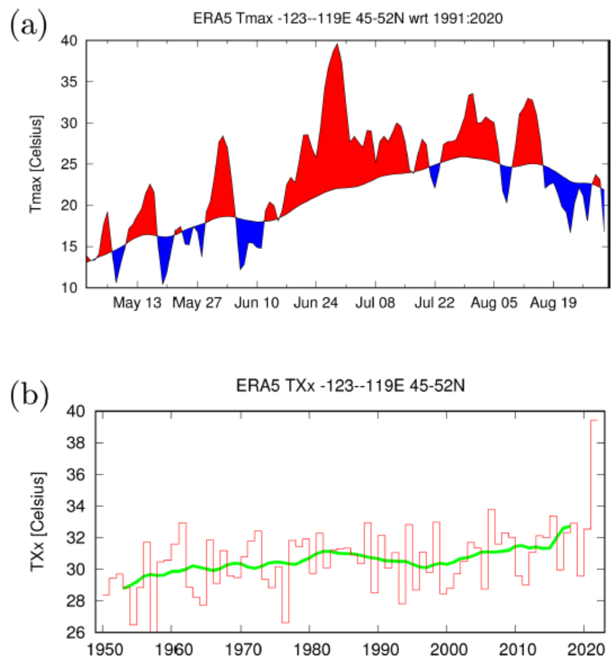

Figure 4. **(a)** Time series for May–August 2021 of the maximum daily temperature averaged over the study area based on ERA5, with positive and negative departures from the 1991–2020 climatological mean of daily maximum temperature shaded red and blue, respectively. **(b)** Annual maximum of the index series with a 10-year running mean (green line). Source: ERA5 (Hersbach et al., 2019).

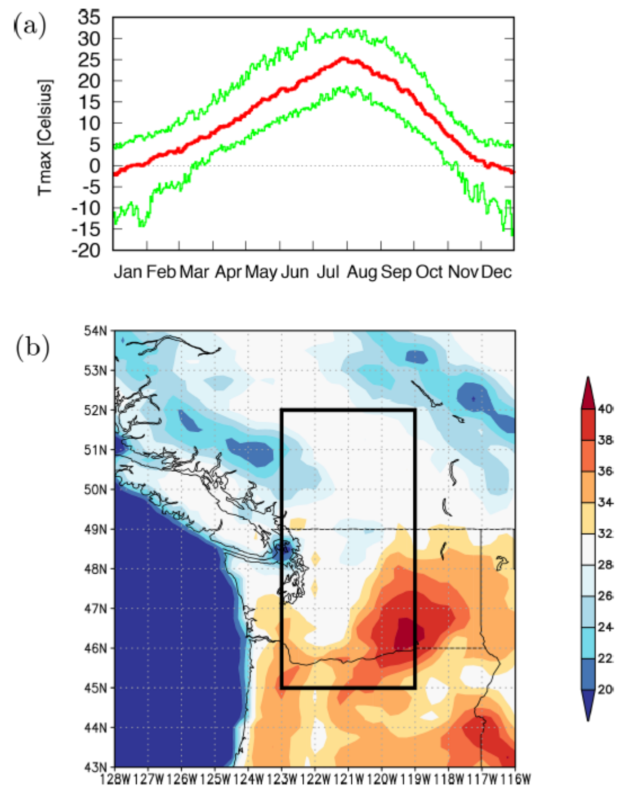

Figure 5. **(a)** Seasonal cycle of Tmax averaged over the land points of 45–52° N and 119–123° N, showing the 1950–2021 mean (red) and 2.5 % and 97.5 % percentiles of the distribution (green). **(b)** Spatial pattern of the 1950–2021 mean of the annual maximum of Tmax (multi-year mean TXx) at each grid point. Source: ERA5 (Hersbach et al., 2019).

mate, but its amplitude would have been increased by climate change in the current climate, which already includes

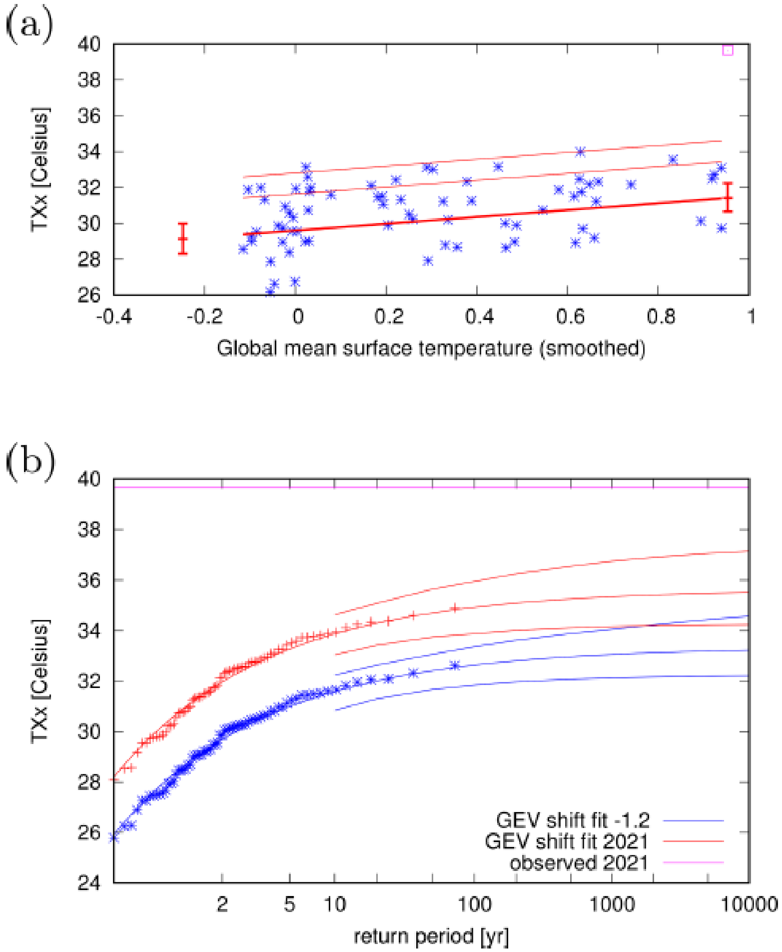

Figure 6. GEV fit with constant scale and shape parameters and location parameter shifting proportional to GMST of the index series. No information from 2021 is included in the fit. **(a)** The observed TXx as a function of the smoothed GMST. The thick red line denotes the location parameter, the thin red lines the 6- and 40-year return period levels. The June 2021 observation is highlighted with the magenta square and is not included in this fit. **(b)** Return period plots for the climate of 2021 (red) and a climate with GMST 1.2 °C cooler (blue). The red and blue lines indicate the best fit and the 95 % confidence intervals; the magenta line shows the observed value. The past observations are shown twice: once shifted up to the current climate and once shifted down to the climate of the late 19th century. Source: ERA5 (Hersbach et al., 2019); fit: KNMI Climate Explorer (https://climexp.knmi.nl, last access: 22 April 2022).

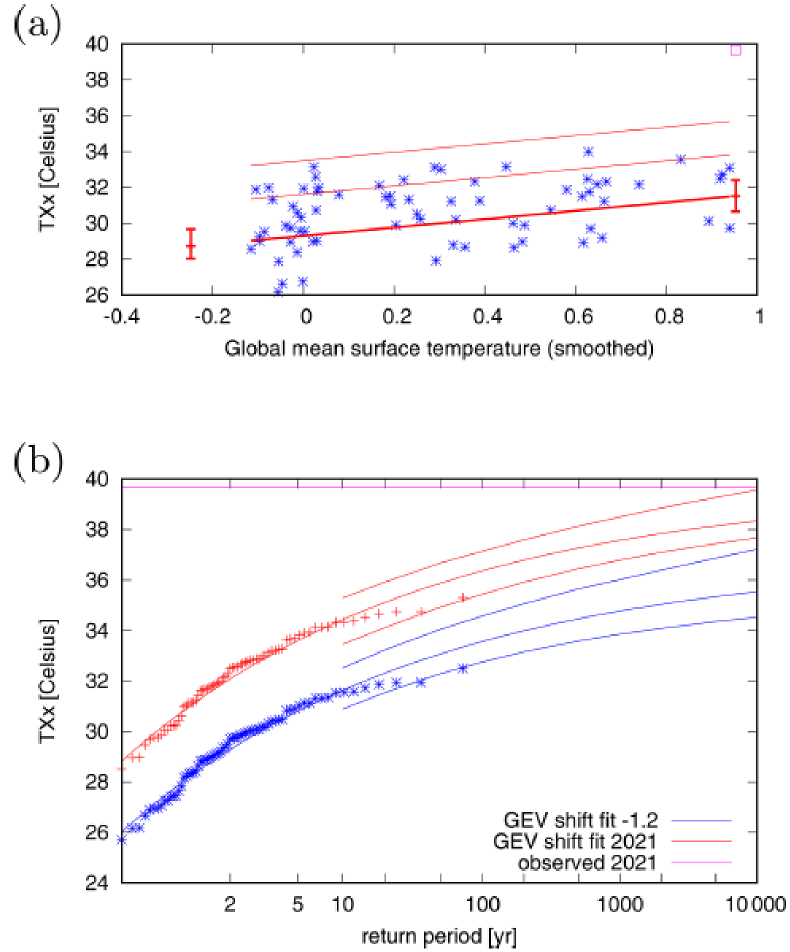

Figure 7. As Fig. 6, but demanding the 2021 event is possible in the fitted GEV function; i.e. the upper bound is higher than the value observed in 2021.

to higher values. The fit also gives a somewhat higher trend parameter.

The third possibility is to fit the GEV distribution over all available data, including observations from 2021 (see Fig. 8). This approach implicitly assumes that the 2021 event is drawn from the same population. We typically do not make this assumption in cases where we intentionally select a specific region in order to maximise the extremity (i.e. return

V. Alternative Methods

Focus on Zhang, Risser, Wehner and O'Brien (*JABES*, 2024)

- Principal idea: analyze individual stations and then combine information (contrast with creating a single region-wide temperature series)
- Temporal covariates:
  - A measure of the combined influence of greenhouse gases
  - ELI (a measure of the El Niño effect)
  - PDSI (measure of drought)
  - "urbanicity"
  - Site-specific "geographical" covariates: latitude, longitude, slope, elevation, distance from coast, mean annual precipitation
- Define $Y(\mathbf{s},t)$ to be maximum at site $\mathbf{s}$ in year t: marginal distribution GEV with parameters $\mu(\mathbf{s},t), \sigma(\mathbf{s},t), \xi(\mathbf{s},t)$ (thin-plate splines for spatial variation, covariate for temporal variation)
- Spatial dependence defined by copula: copula of $Y(\mathbf{s},t)$ assumed to be the same as that of $X(\mathbf{s},t)$, a process of form

$$X(\mathbf{s},t) \quad = \quad R_t W(\mathbf{s},t) + \epsilon(\mathbf{s})$$

  where R_t are independent Pareto RVs with index $\frac{1-\delta}{\delta}$ ($\delta \in (0,1)$), $W(\mathbf{s},t)$ is an isotropic spatial Gaussian process transformed to Pareto margins with index 1, and $\epsilon(\mathbf{s})$ are independent Gaussian RVs for each $\mathbf{s}$
- Granger causality: counter-factual based on greenhouses gases c. 1950

Results and Discussion

L. ZHANG ET AL.

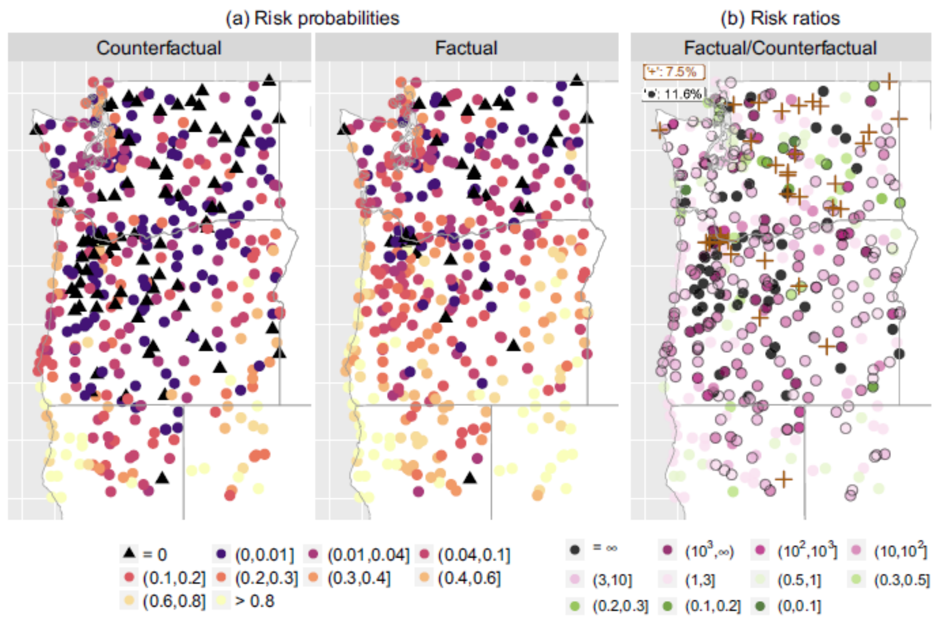

Figure 4. Subfigure a shows the station-specific posterior medians of the risk probabilities calculated from statistical model M4 for the Counterfactual (left) and Factual (right) climate scenarios, and subfigure **b** shows their ratio. For the risk probabilities, solid black triangles indicate gauged locations for which the risk probability best estimate is zero; for the risk ratios, solid black circles denote $RR(s) = \infty$ (wherein the counterfactual risk probability is zero but the factual risk probability is nonzero) and yellow '+' shows where the risk ratios are undefined (wherein both counterfactual and factual risk probabilities are zero). In the rightmost panel, points that are plotted with additional 'o' sign indicates that risk ratio estimates are statistically significantly different from 1 .

- Analysis confined to 438 "homogeneous" stations in US
- Typical estimated risk ratios between 3 and 10, but still some that are < 1 or $+\infty$
- Very computationally intensive fitting procedure!
- Does a much better job of accounting for the observed temperatures, but broader interpretation still unclear

VI. Examples

- Renalyze data of Philip *et al.* (2022)
- Data: Daily maximum near-surface air temperature 1950–2021, averaged over longitudes 123.125 to 118.875°W, latitudes 44.875 to 52.125°N. Also annual maxima
- Fit GEV to annual maxima, with GMST as a covariate:

$$\mu_t = \beta_0 + \beta_1 \mathrm{GMST}_t, \ \sigma_t = \sigma, \ \xi_t = \xi,$$

Parameter	Excluding 2021 Estimate	Excluding 2021 Standard error	Including 2021 Estimate	Including 2021 Standard error
β_0	29.720	0.286	29.242	0.284
β_1	1.758	0.548	2.595	0.641
σ	1.729	0.174	1.694	0.148
ξ	–0.469	0.085	–0.128	0.055

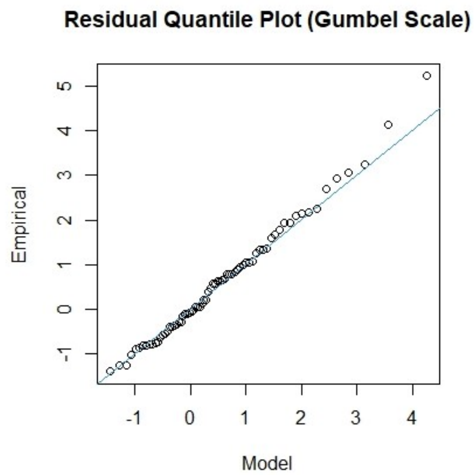

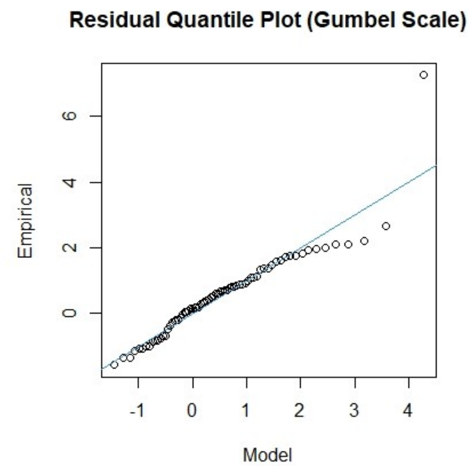

Conclusions derived from annual maxima analysis

- Define "factual" (F) and "counterfactual" (C) scenarios as $GMST_{2021}$ and $GMST_{2021} - 1.2$ on basis of 1.2°C overall warming
- Endpoints $\omega_F = \beta_0 + \beta_1 GMST_{2021} - \sigma/\xi$ and $\omega_C = \beta_0 + \beta_1(GMST_{2021} - 1.2) - \sigma/\xi$.
- Estimate $\hat{\omega}_F = 35.05$ (SE=0.61) and $\hat{\omega}_C = 32.94$ (0.40), almost the same as Philip *et al.* (2022) (note: observed value was 39.6°C).
- Bayesian analysis shows $\Pr\{\omega_F > 39.6\} \approx 0.0088$ and $\Pr\{\omega_C > 39.6\} \approx 0.0025$, but this is not easily translated into a statement about relative risk

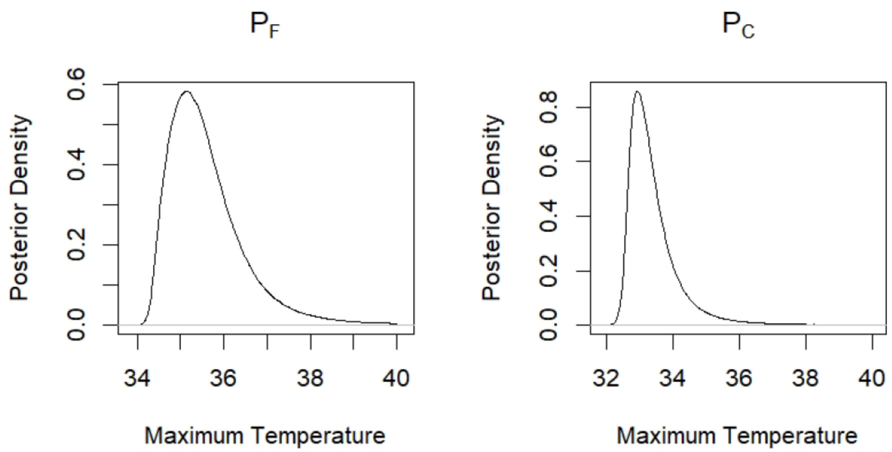

FIGURE 2
Posterior density of the maximum temperature under factual (P_F) and counterfactual (p_C) models.

Alternative "threshold exceedances" approach

(Clarkson et al. (2023), *Applied Statistics* **72**, 829–843)

- Basic idea: model all exceedances above a threshold. Since the temperature series is heavily seasonal, the threshold must be seasonal as well
- Selecting the threshold: use quantile regression to define threshold u_t at time t, as a function of sinusoidal terms and a nlinear time trend
- Declustering based on the extremal index (Ferro and Segers 2003)
- Fit the point process model (`pp.fit` in ismev) to data from May 15–September 15 each year, estimate time-varying parameters μ_t, σ_t, ξ, where μ_t depends on $GMST_t$
- Estimated endpoints are larger than before, but still less than the observed value 39.6°C
- Bayesian analysis to estimate exceedance probabilities p_F and p_C for a sequence of thresholds

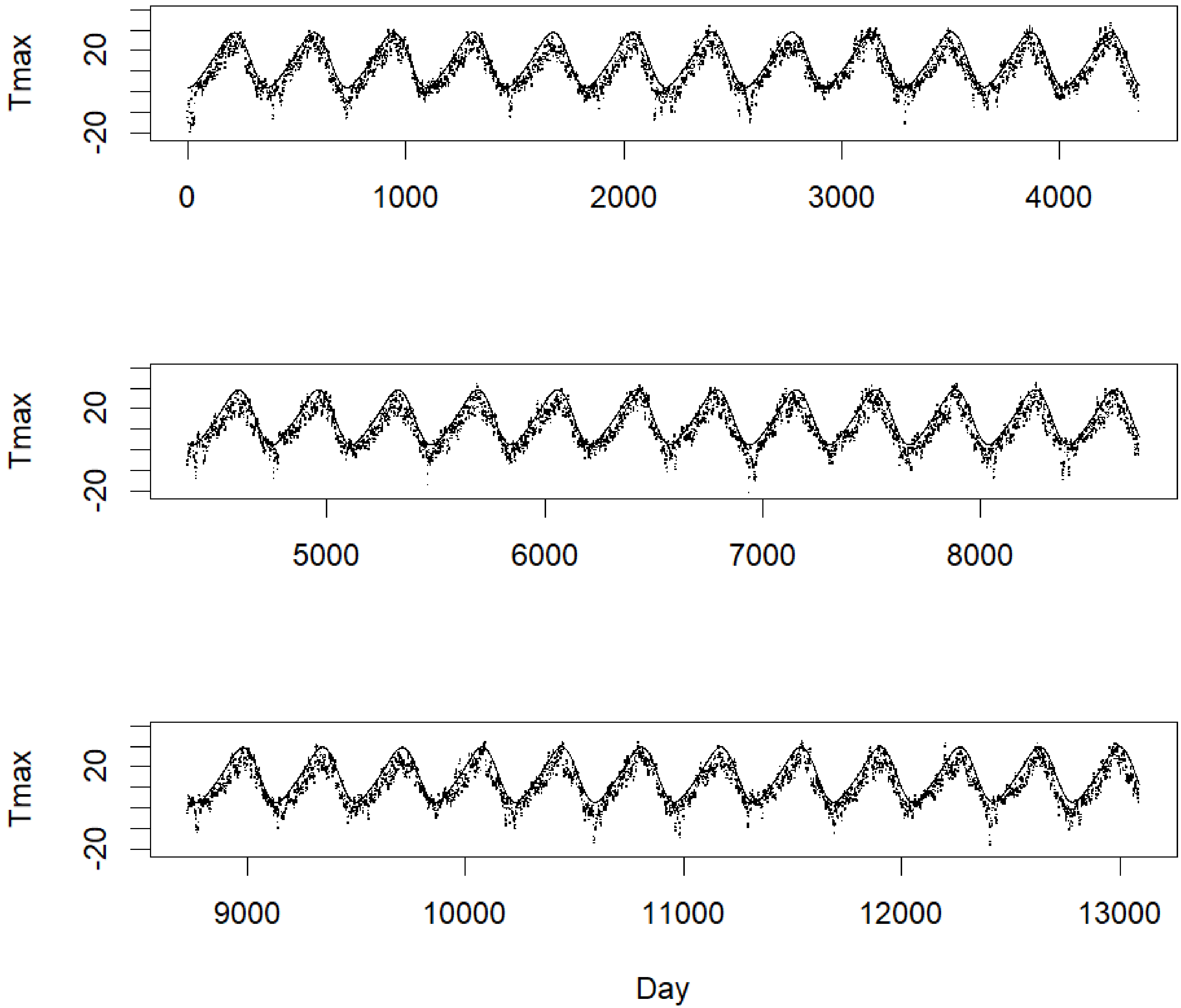
Tmax
20
-20
0
1000
2000
3000
4000
Tmax
20
-20
5000
6000
7000
8000
Tmax
20
-20
9000
10000
11000
12000
13000
Day

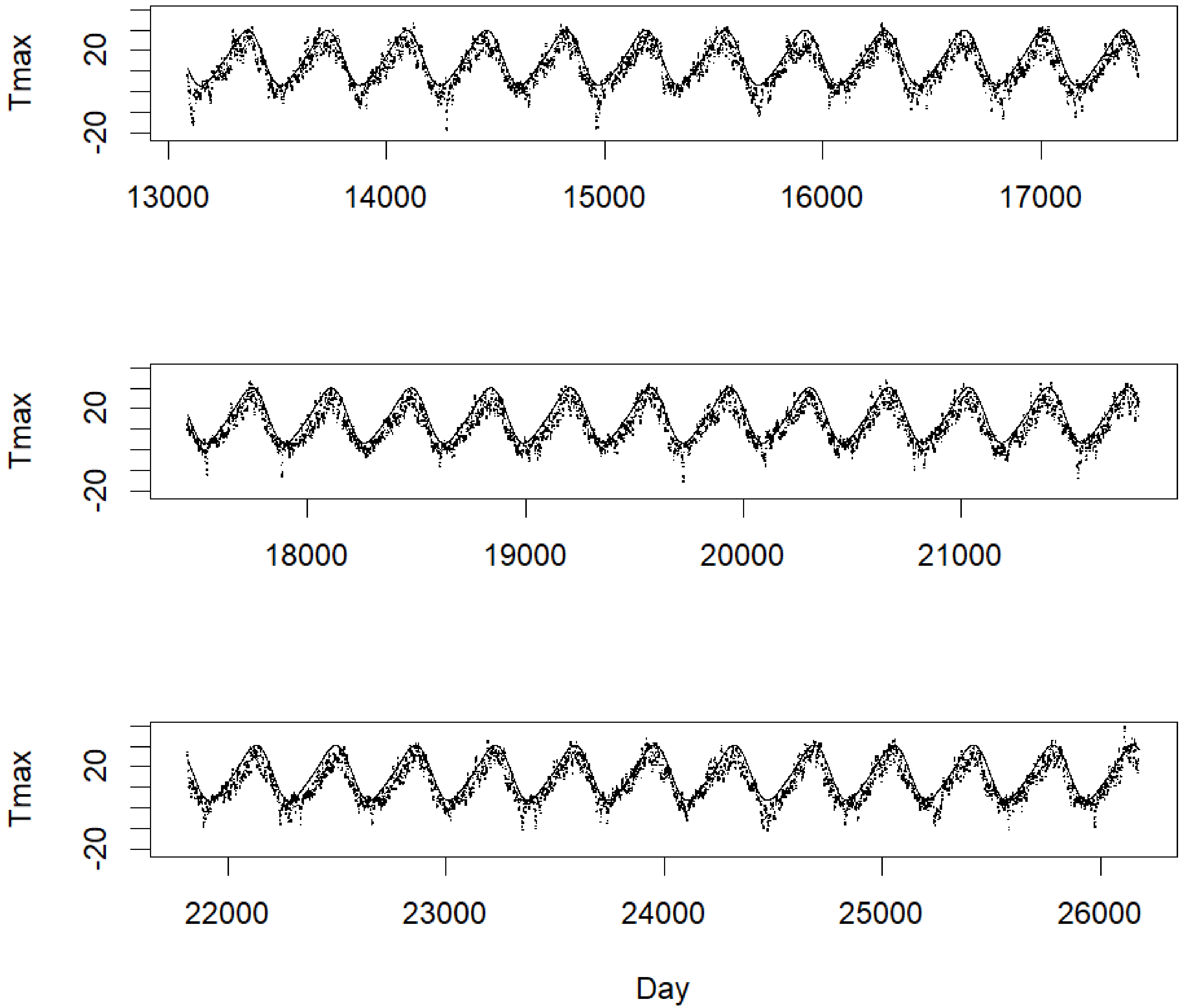
Tmax
20
-20
13000
14000
15000
16000
17000
18000
19000
20000
21000
22000
23000
24000
25000
26000
Day

Results of Bayesian threshold analysis

Temp. °C	$E\{p_F\}$	$E\{p_C\}$	$E\{p_C/p_F\}$	$q_{0.025}$	$q_{0.975}$	Pr $\{p_C/p_F < 0.01\}$
34	0.122	0.0022	0.020	0	0.132	0.65
35	0.031	2.1×10^{-4}	4.8×10^{-3}	0	0.053	0.901
36	4.8×10^{-3}	2.0×10^{-5}	1.4×10^{-3}	0	0.0013	0.971
37	5.0×10^{-4}	2.7×10^{-6}	6.4×10^{-4}	0	0.00083	0.988
38	4.9×10^{-5}	4.8×10^{-7}	3.6×10^{-4}	0	0	0.994
39	5.3×10^{-6}	1.0×10^{-7}	2.1×10^{-5}	0	0	0.996

- p_F and p_C are probabilities that the annual maximum is more than "Temp." under factual and counterfactual models
- "Factual" model assumes $GMST_{2021}$; "counterfactual" assumes $GMST_{2021} - 1.2$
- $q_{0.025}$ and $q_{0.975}$ are quantiles of the posterior distribution of p_C/p_F
- Last column represents posterior probabilities

Takeaways

- The 2021 event was particularly extreme, but there will surely be others that are equally problematic

- Some statistical methods do better than others
  - GEV with covariates: fails if observed event beyond estimated end-point of distribution
  - Bayesian methods, threshold approach: better, but may not resolve fundamental problem
  - Fully spatial analysis: potentially best method, expensive to implement, complicated to explain

- Physical explanations?
  - "Heat dome" event: but still need to quantify

- Maybe need to change formulation of the problem, e.g.
  - Focus on thresholds less extreme than the observed event
  - Greater use of Bayesian posterior intervals to quantify uncertainty